Sound Measurement as a Means of Gas-Bubble Sizing in Aerated Agitated Tanks

Jonathan W. R. Boyd and Julie Varley
Biotechnology and Biochemical Engineering Group, University of Reading, Reading, U.K.

Bubble size affects mass transfer and mixing hydrodynamics significantly in a gas–liquid agitated vessel. It is important that accurate and reliable techniques are developed to measure bubble size to improve design and scale-up of such vessels. Existing bubble-size measurement techniques are time-consuming (e.g., photography) or complex and expensive (e.g., ultrasound). The ideal technique, capable of on-line measurement in any type of liquid, has yet to be developed. It is possible to size gas bubbles from sound measurement within a gas-sparged agitated tank. A significant amount of the noise, measured close to the impeller, is made up of transient, damped, sinusoidal pressure pulses, which are heard only in the presence of gas bubbles. Analysis of the individual sound pulses in terms of magnitude, frequency and damping, combined with photographic validation, indicates that the sound is caused by bubbles oscillating at frequencies dependent on bubble size. The bubbles are excited into oscillation when formed at the impeller. Sound from other sources (e.g., turbulence) is differentiated from bubble sound. Theoretical modeling and experimental results are used to estimate the sound contribution of a single bubble to a sound spectrum and calculate the bubble-size distribution at the impeller directly from experimentally measured sound-pressure spectra.

Introduction

Gas-sparged agitated vessels are used in the chemical and biotechnology industries extensively as reactors and mixing vessels. Organism growth and product formation in bioreactors can be limited by the rate of mass transfer from the gas phase into the liquid phase. The interfacial area available for mass transfer across the two phases and the bubble-size distribution are important factors when designing an impeller-agitated bioreactor. Most research in this area has concentrated on measuring the global interfacial area and bubble Sauter mean diameter to produce semiempirical correlations relating bubble size to power consumption for design purposes.

Gas-bubble size has a significant effect on the mass transfer, mixing hydrodynamics, and power input. Changes in process conditions or changes in the physical properties of the system have an effect on bubble size. The importance of gas-bubble size has led to the development of several different methods of bubble-size measurement. Gas bubbles in transparent fluids can be photographed and their size measured, usually using image-analysis software (e.g., Machon et al., 1997). This is the simplest technique but cannot be used with opaque media such as those found in fermentation systems. Probes, relying on the conductive, dielectric, or optical properties of the liquid media, measure bubble penetration or chord lengths (Saxena et al., 1988). Statistical models (e.g., Clark and Turton, 1988) are required to calculate bubble-size distributions from the measured chord lengths. An isokinetic probe removes a small, constant stream from the gas–liquid dispersion, and the lengths of bubble slugs formed in a capillary are measured using photoelectric detectors allowing bubble volumes to be calculated (Greaves and Kobbacy, 1984; Barigou and Greaves, 1992; Lu et al., 1993; Lu and Lin, 1995). Although the use of probes allows the spatial variation of bubble size within a vessel to be measured, they interfere with the flow pattern of the dispersion and the bubbles being measured. Small bubbles (less than 2 mm) are difficult to measure and the Sauter mean diameter is often underestimated. The use of ultrasound as an analytical tool has become common (McClements, 1997) and the disadvantages of probes has led to development of various ultrasound bubble-

Correspondence concerning this article should be addressed to J. Varley.

size measurement techniques (Chapelon et al., 1985; Stravs and Von Stockar, 1985; Stravs et al., 1986; Bugman and Von Stockar, 1989; Leighton et al., 1991; Vagle and Farmer, 1992). These techniques are reviewed by Leighton et al. (1997). Only one ultrasound technique has been applied to a fermenter system (Stravs et al., 1986), and this was used to measure gas interfacial area and not bubble size. Ultrasound techniques to measure bubble-size distributions in a fermenter have not as yet been developed and involve complex and expensive equipment. Some ultrasound techniques have limitations on the size range of bubbles that can be measured.

The ideal bubble-size measurement technique would be of use in any real system and would be capable of measuring a wide range of bubble sizes with minimum intrusion. Real-time, on-line measurements would be advantageous for control purposes, especially in a fermentation process where changing solute concentrations are likely to affect bubble size. It is obvious that as yet no one technique is capable of fulfilling all these requirements. Therefore, there is a need to develop further accurate and reliable bubble-size measurement techniques.

The long-term objective of the studies described here is the development of an uncomplicated technique to measure bubble size in a gas–liquid dispersion from the sound pulses emitted from bubbles that are audible by the human ear, that is, *passive acoustic emissions*. Simple sound measurement is a far less complex technique than ultrasound, taking advantage of a process occurring naturally within the mixing vessel. Bubble-volume oscillations can create very high sound pressure magnitudes at frequencies dependent on the bubble radius (Minnaert, 1933; Strasberg, 1953, 1956). Minnaert (1933) calculated the frequency of bubble oscillation in a free field to be:

$$f_0 = \left(\frac{3\gamma P_0}{\rho}\right)^{0.5} \frac{1}{2\pi a}, \tag{1}$$

where f_0 is the natural frequency of bubble oscillation, γ is the ratio of specific heat capacities, P_0 is the pressure of the surrounding liquid, ρ is the liquid density, and a is the bubble radius. Plesset and Prosperetti (1977) showed that the natural frequency of bubble-volume oscillation also depends on surface tension. However, for an air–water system the effect of surface tension on frequency is generally assumed negligible for bubbles greater than 0.1 mm in radius. If the surface tension of a liquid is reduced by 50%, the natural frequency of a 2-mm-diameter bubble would decrease by only 6×10^{-5}%, and therefore surface tension can be ignored for fermenter media. For large bubbles, shape oscillations can also be excited at the same time as volume oscillations, but these modes of oscillations are radiated less efficiently and the pressures involved are significantly less than those for volume oscillations (Strasberg, 1956).

Sound due to the gas sparging in an agitated vessel has been investigated previously by Hsi et al. (1985), Ursy et al. (1986), Sutter et al. (1987), and De More et al. (1988), but these studies concentrated on low-frequency sound. The peaks in the sound spectrum were used to identify the type of ventilated gas cavities formed in the low-pressure regions behind the impeller blades of a Rushton turbine, particularly the 3–3 cavity structure where 3 large and 3 clinging gas cavities exist. Also, the magnitude of certain peaks was related to mass transfer. It was suggested that the higher frequency sound was due to volume oscillation of gas bubbles at their natural frequencies. However, the individual bubble sound pulses measured by Medwin and Beaky (1989), Updegraff and Anderson (1991), and Kolaini and Crum (1994) in breaking laboratory and sea waves were not identified in the studies involving an agitated vessel.

Sound measurement has been used previously to size bubbles in gas–liquid systems other than agitated vessels. Leighton and Walton (1987) counted and analyzed the bubble-pressure pulses from sound pressure–time measurements in a flowing brook to produce size distributions of the entrained gas bubbles. Pressure–time traces and sound spectra have been used to size single bubbles formed at a nozzle at moderate to high bubbling rates (Manasseh, 1996). Loewen and Melville (1991) developed a model for the sound production in a breaking ocean wave based on individual bubble oscillations and used this model to suggest a method for calculating bubble-size distributions from sound spectra. Pandit et al. (1992) used the same technique to calculate bubble-size distributions from the sound spectra produced by a gas–liquid jet mixer and flow in a horizontal pipe and, although the theory of the mechanisms of sound production differ from those proposed by Loewen and Melville (1991), obtained good results when the calculated bubble-size averages and standard deviations were compared with photographic measurements. Pandit et al. (1992) assumed that the bubbles were excited into oscillation by uniform turbulence, predicting, from theory, pressure magnitudes an order of magnitude higher than those measured by other investigators of bubble sound, such as Medwin and Beaky (1989). Comparison of the experimental sound measurement results by Pandit et al. (1992) with other studies cannot be made, as the sound pressure spectra results were only presented with arbitrary units and the individual bubble oscillations were not shown.

This article validates a novel, uncomplicated technique for measuring for bubble-size distribution from a measured sound spectrum in a gas–liquid dispersion. The case of a gas-sparged agitated vessel is investigated here but, in principle, the technique could be adapted to other gas–liquid systems. Analysis of hydrophone measurements at the impeller region of the agitated vessel showed that bubble oscillation accounts for a significant amount of high-frequency sound. Other sound sources are identified and differentiated from bubble sound. By modeling the sound production processes in the vessel, it has been established that the bubbles oscillate at or near their natural frequencies, which are dependent on bubble size. After removal of nonbubble sound, experimentally measured sound spectra (sound pressure vs. frequency) are then used to calculate the bubble-size distribution. These calculations are validated using photographically measured size distributions. The importance of understanding the exact causes of bubble sound is discussed, as this has direct implications on whether the technique can be validated with photographically measured distributions and the improvement of the technique's accuracy.

Experimental Study

The mixing vessel, shown in Figure 1, was a clear 98-mm-diameter cylindrical plastic tank of standard geometry. The

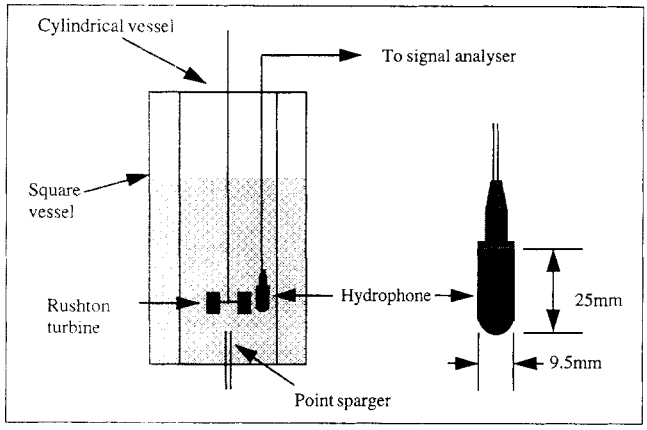

Figure 1. Mixing vessel and hydrophone.

tank was filled to 196 mm in height with deionized water. The tank was agitated by a RW 20 DZM Ika-labortechnik stirrer with a 48-mm-diameter Rushton turbine, 6.5 mm above the tank base. Photographs were used for validation of bubble size, so the cylindrical vessel was surrounded by a clear plastic 130-mm square tank, which was also filled with the water to minimize the distortion in photographs due to the curvature of the vessel wall. The agitation rates were varied between 200 and 1,600 rpm. Gas was sparged into the vessel through a glass tube (3 mm internal diameter), 30 mm below the impeller, and gas flow rates measured using a standard Platon flowmeter were between 60 and 600 $cm^3 \cdot min^{-1}$. Gas flow rates were deliberately kept low to ensure accuracy in the photographic bubble-size analysis, used for validation.

Sound pressure was measured using a 8103 Bruel and Kjaer hydrophone with a frequency response from 0.1 kHz to 200 kHz and receiving sensitivity of 27.2 μV/Pa. The receiving signal was amplified using a Kistler 5011 preamplifier and then stored and analyzed using a Hewlett-Packard 35660A Dynamic Signal Analyzer capable of performing fast Fourier transformations (FFTs). Time-record lengths of 0.0039 s to 2048 s were possible. The most suitable time length for looking at the widest range of individual bubble oscillations was found to be 15.6 ms. This time span gave a frequency spectrum that spanned 0 to 25.6 kHz. However, sound at frequencies greater than 25.6 kHz was measured using smaller time spans. Sound spectra were made up from the average of 400 time records. The hydrophone was positioned 5 mm away from the impeller tip to capture the sound of bubbles as they were formed and to measure the lower frequency gas cavity sound for comparison with the work of Hsi et al. (1985), Ursy et al. (1986), and Sutter et al. (1987), which were carried out at a different scale.

The spectrum analyzer was only capable of basic signal analysis, so the measurement data were transferred to a Sparc workstation where further calculations were performed using Matlab 5. The Matlab 5 Signal Analysis Toolbox is capable of FFT analysis and allows filtering or removal of unwanted frequencies from the sound signal. Matlab 5 was also used for the modeling calculations and bubble-size calculations.

Bubble sizes were measured from photographs of the impeller region using PC_Image (Foster Findlay Associates) for comparison with acoustic results. The system was calibrated from photographs of a ruler placed inside the vessel. The bubbles were assumed ellipsoidal in shape and therefore an equivalent bubble diameter was used. The maximum and minimum chords were measured and the bubble's third dimension was taken to be the same as the larger of the two chord measurements. The equivalent diameter was taken to be a geometric average of the three dimensions.

Pressure–Time Traces

Figure 2 shows four examples of pressure–time records measured at the tip of the impeller. Trace I shows a 15-ms pressure–time trace as the impeller blades pass the hydrophone at an agitation rate of 800 rpm but without gas sparging. Only the low-frequency pressure changes due to the blade passing the hydrophone, and the turbulent eddies can be seen. Traces II and III show examples of 15-ms time records at the same agitation rate but sparged with 300 cm^3 min^{-1} of air. Comparing Traces I, II and III it can be seen that superimposed onto the low-frequency ungassed trace there are transient, high-frequency pressure pulses. A general example of an individual pulse not overlapping any other pulses is shown more clearly in Trace IV. The pulse starts with a small peak in pressure (point A), and then there is a large drop in pressure (point B), after which the magnitude of the oscillations decreases with time. The oscillation of an individual pressure pulse occurs at a constant frequency. These pulses were not seen in the ungassed case, so the likely cause of the sound was the introduction of gas bubbles. The frequencies of the pressure pulses, observed in 15-ms time records, range from 900 Hz to 30,000 Hz. Using Eq. 1 and assuming that $P_0 = 1 \times 10^5$ Pa, $\gamma = 1.4$ for adiabatic compression, and $\rho = 1000$ kg^{-3}, then these frequencies would correspond to spherical bubbles of diameters 7.2 and 0.2 mm, respectively, oscillating adiabatically at their natural frequencies. Bubbles of this size were photographed in the vessel around the impeller region. Similar transient pulses due to bubble-volume oscillation were observed by Medwin and

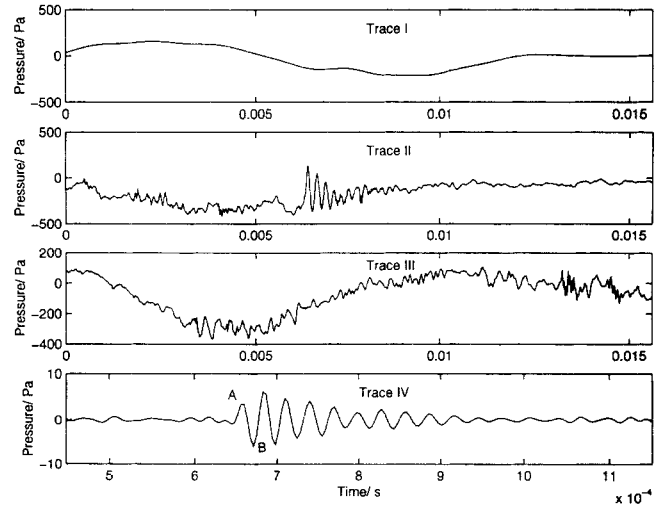

Figure 2. Sound pressure–time records measured 5 mm from the tip of Rushton turbine.

Trace I: 0.0156 s; ungassed, $N = 800$ rpm. Traces II and III: 0.0156 s; sparged, $N = 800$ rpm and $Q = 300$ $cm^3 \cdot min^{-1}$. Trace IV: Enlarged example of a typical pulse shown over 6×10^{-4} s.

Beaky (1989), Updegraff and Anderson (1991), and Kolaini and Crum (1994) when measuring sound due to the entrainment of air bubbles as a wave broke at the surface of the sea.

If the initial amplitude of the bubble-volume oscillation is very small, then a bubble oscillates in an exponentially damped sinusoidal manner (Strasberg, 1956), like a spring or pendulum. This can be described by the following simple equation (Updegraff and Anderson, 1991):

$$p = p_0 \sin(2\pi ft) e^{-(\beta t)}, \tag{2}$$

where p is the pressure at the hydrophone at time, t; p_0 is the initial pressure magnitude of the bubble oscillation; and β is the exponential decay constant ($= \pi f \delta$).

The energy losses due to thermal conduction between the gas and surrounding liquid, work done against viscous forces at the bubble wall, and energy lost as an acoustic wave (Strasberg, 1956; Devin, 1959; Eller, 1970), are accounted for by the dimensionless constant δ. For a clean spherical air bubble in water (Strasberg, 1956):

$$\delta = 0.014 + 4.5 \times 10^{-4} \sqrt{f}. \tag{3}$$

After removal of low-frequency sound from the time traces using filters, the exponential decay constant, β, of nonoverlapping pressure pulses was calculated using the method of successive oscillations described by Devin (1959). Figure 3 shows how the experimentally measured β for many pressure pulses, under various gas flow and agitation rates, compares with theoretical values calculated using Eq. 3. The measured damping of the pulse oscillations is in general agreement with that predicted using Eq. 3 for an oscillating spherical bubble. Therefore, the likely source of these transient pulses is bubble oscillation. This slight increase in experimentally measured damping constants from theory has been observed by previous studies (Strasberg, 1956; Devin, 1959; Medwin and Beaky, 1989), suggesting that damping mechanisms other than those just accounted for theoretically can exist. Longuet-Higgins (1992) proposed that there could be a transfer of energy between the bubble-volume oscillations and their shape oscillations causing increased damping. In the turbulent stream behind the impeller blade, bubbles are constantly changing shape and this could lead to the increased damping of the volume oscillations observed experimentally in Figure 3.

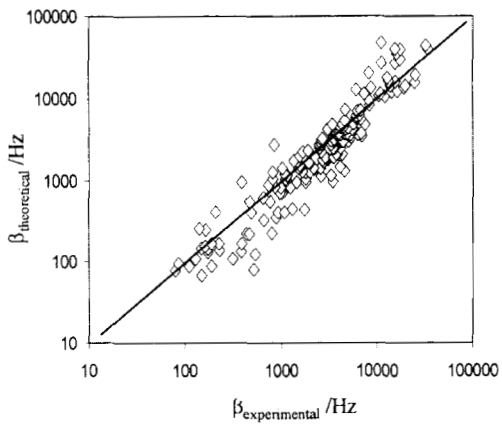

Figure 3. Experimental vs. theoretical bubble oscillation exponential damping constants ($\beta = \pi f \delta$).

They were measured at agitation rates between 200 and 800 rpm, and at gassing rates between 100 and 500 $cm^3 \cdot min^{-1}$.

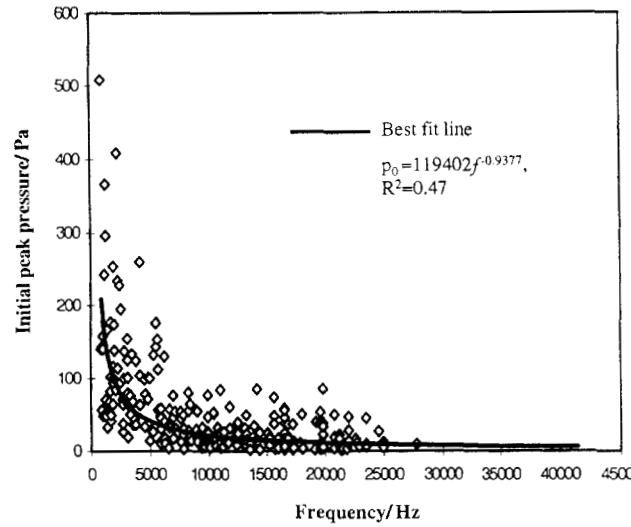

Figure 4. Scatter plot of initial peak-pressure magnitudes of bubble oscillations measured at hydrophone.

Figure 4 shows a scatter plot of initial magnitudes of over 300 pressure pulses against their frequency of oscillation measured 5 mm from the impeller at an agitation rate, N, of 800 rpm and gas flow rate, Q, of 300 $cm^3 \cdot min^{-1}$. The initial peak magnitude is dependent on the distance at which the measurements are being taken and the mechanisms that cause the bubbles to oscillate (Strasberg, 1956). It can be seen that the lower frequency oscillations have significantly higher peak-pressure magnitudes. It is likely that the sound from larger bubbles is easier to detect, as the higher frequency sound from the smaller bubbles tends to be scattered and absorbed by other bubbles, as suggested by Kolaini and Crum (1994). Updegraff and Anderson (1991) measured peak pressures from 0.2 Pa to 1.2 Pa at a distance of 1 m due to oscillations produced by bubbles, approximately 0.8 to 6 mm in diameter, entrained in a breaking wave. The measured peak magnitudes shown in Figure 4 at the impeller range from 5 Pa to 500 Pa and are plausible values when compared to the results of Updegraff and Anderson (1991), as they have been measured at distances one to two orders of magnitudes nearer the sound source.

When the hydrophone was moved away from the impeller region, the number and magnitude of high-frequency pulses measured were significantly reduced. Therefore, it seems that the bubble oscillations are excited in the region around the impeller and the sound measured is local to that area.

Prediction of these initial peak-pressure magnitudes from theory is difficult because of the many processes involved in exciting the bubbles into volume oscillations. Pumphrey and Ffowcs Williams (1990) review four possible causes exciting a bubble into oscillation for bubbles entrained at the surface of the sea:

1. Uniform pressure change over the surface of the bubble, for example, the change in hydrostatic pressure as the bubble rises;

2. Existence of a radial wall velocity when the bubble is formed;

3. Shape oscillations may be in resonance with the volume oscillations;

4. Pressure changes due to liquid turbulence.

All these processes exist within an agitated tank and the cause of bubble-volume oscillation could be predominantly one or a combination of two or more of them. The bubble-volume oscillations are so small that they have only been observed optically using laser light and photodetectors (Stroud and Marston, 1993). The displacement of the bubble radius from its equilibrium has been estimated to be of the order of 10^{-8} m for a 1-mm-diameter bubble (Leighton and Walton, 1987). These small displacements exist at the same time as the more visible shape oscillations, so there is little chance of understanding the causes of bubble pulsation through visual experimental techniques. It is perhaps only through experimental sound measurement and theoretical analysis that the processes involved can be inferred. Referring to Figure 2, Trace IV, in which an example of an individual pulse is shown, the initial peak in pressure (point A) suggests that the bubble's volume expands slightly, initiating a much larger compression, followed by the damped, simple harmonic oscillation. It is difficult to envisage a bubble hit by a turbulent eddy initially expanding, so this type of pressure pulse is unlikely to be caused by turbulence, and bubble breakage is therefore the more likely cause of bubble oscillation.

Sound Spectra

Figure 5 shows a comparison of the sound spectrum measured at the impeller of an unsparged agitated vessel (800 rpm) and the spectrum when the vessel is sparged with 300 $cm^3 \cdot min^{-1}$ of gas. As was seen earlier in the analysis of the time traces, there is no significant sound above 500 Hz in the ungassed conditions. Under gas-sparged conditions, however, there is a significant amount of sound above 900 Hz in the spectrum. Also the magnitude of low-frequency sound below 500 Hz has been increased. Figure 6 shows low-frequency sound under gassed conditions up to 400 Hz for the same conditions as Figure 5. Imposed on the background noise due to turbulence ranging between 0 and 400 Hz, significant peaks are observed at the blade passing frequency of 80 Hz (peak A) and its second fundamental of 160 Hz (peak B). Hsi et al. (1985), Ursy et al. (1986), and Sutter et al. (1987), in a 900-mm-diameter vessel, measured a second set of harmonics at multiples of 1.5 times the blade passing frequency when 3–3 cavity structures existed behind the impeller blades. This second set of harmonics was not observed in these studies. Two clear regions in the sound spectra can be seen: a low-frequency region due to turbulence and the impeller blade passing the hydrophone below 900 Hz, and a high-frequency region due to the introduction of gas into the vessel above 900 Hz. Low-frequency sound due to collective bubble oscillation, as investigated by Yoon et al. (1991) and Nicholas et al. (1994), was also expected between 0 and 1,000 Hz, particularly if the hydrophone was positioned further away from the main region of sound near the impeller. In this case, however, no spectral peaks could be identified as being due to collective bubble sound, even when sound measurements were made from outside the agitated vessel.

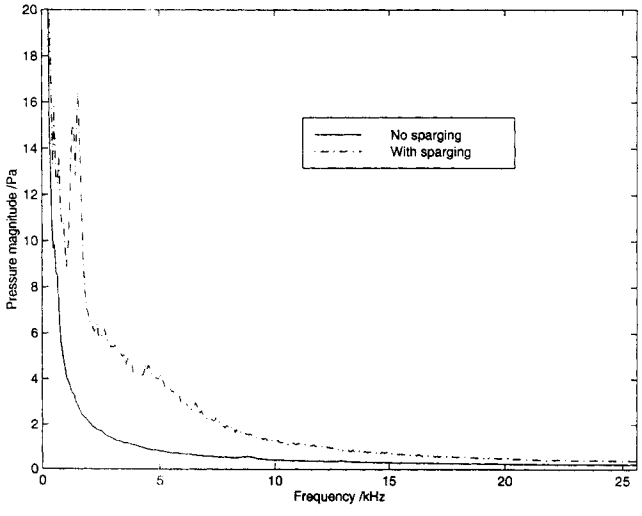

Figure 5. Sound spectra measured at impeller tip with: unsparged (trace A, $N = 800$ rpm) and sparged (trace B, $N = 800$ rpm, $Q = 300$ $cm^3 \cdot min^{-1}$) conditions.

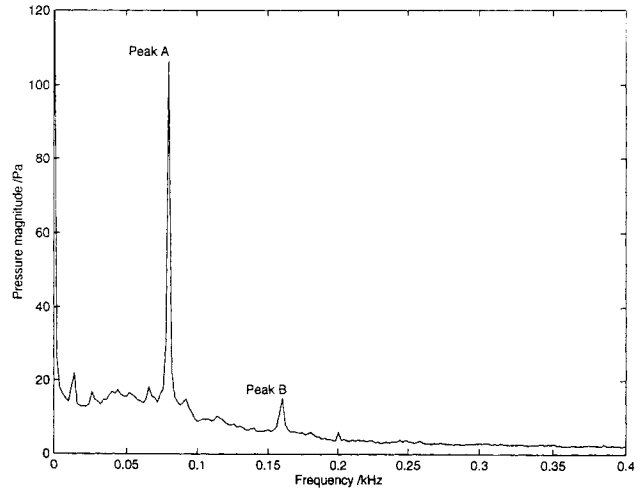

Figure 6. Low-frequency sound spectrum under gassed conditions ($N = 800$ rpm, $Q = 300$ $cm^3 \cdot min^{-1}$).

Peak A corresponds to the impeller-blade passing frequency. Peak B corresponds to twice the blade passing frequency.

Figure 7 shows the variation in the high-frequency spectra with agitation rate, N, with the gas sparging rate, Q, kept constant at 100 $cm^3 \cdot min^{-1}$. Two spectra are shown for each of the conditions to demonstrate the reproducibility of the sound measurements. Spectrum A shows sound due only to gas being sparged into the vessel. There is sound due to tank resonance below 0.5 kHz and some sound around 0.95 kHz due to bubbles of approximately 7 mm in diameter being sparged into the vessel (estimated from bubble formation rate at the nozzle measured from time traces and constant gassing rate). At 200-rpm (spectrum B) bubbles were just beginning to be broken up. Bubbles were not being recirculated to the

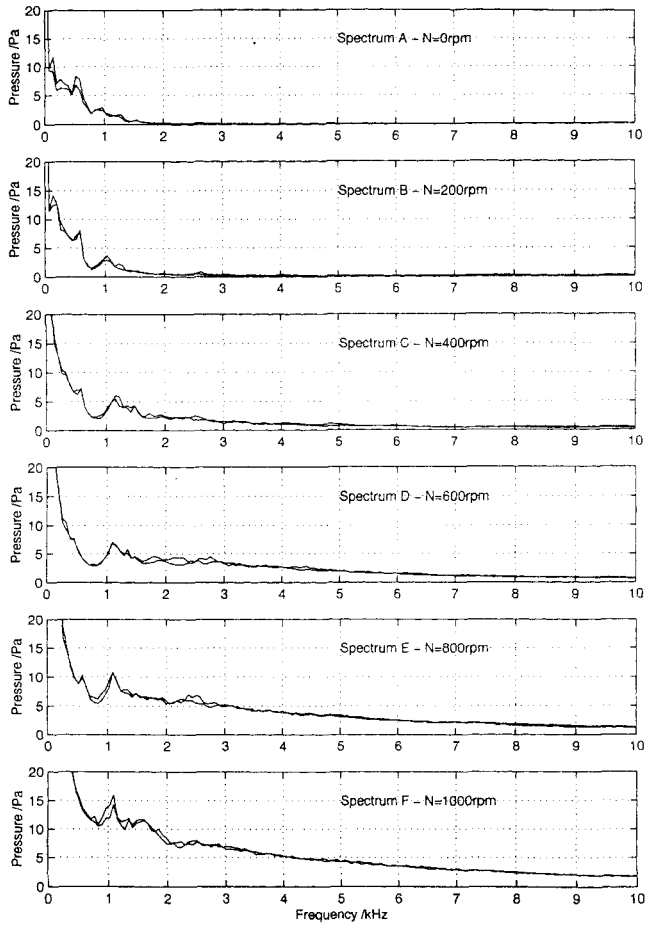

Figure 7. Effect of increase in agitation on high-frequency sound spectra.

Two spectra are shown at each agitation rate to demonstrate repeatability.

impeller, and with an impeller Reynolds number ($= \rho ND^2/\mu$) below 10^4, turbulent flow in the tank was not fully established, so the low-frequency sound was still mainly due to tank resonance. As agitation rate (spectra C–F) increases, so too does the magnitude of sound at higher frequencies due to more bubbles being formed at the impeller per unit time. Also more sound is observed at higher frequencies as smaller bubbles form. Hsi et al. (1985) suggest that some of the high-frequency sound is due to small-scale turbulent eddies. For the scale of equipment used in these studies this is unlikely, as the frequency of turbulent eddies [estimated by Kolmogorov's theory of isotropic turbulence (Kawase and Moo-Young, 1990)] are of an order of magnitude lower than those of bubble oscillations, as the gas bubbles in this case are quite small in comparison to those observed by Hsi et al. (1985). Low-frequency sound increases due to the development of turbulence and, as the blade passing frequency increases, this low-frequency band moves toward the region of bubble sound. This may mean that there is a limiting agitation rate for the measurement technique, above which bubble sound cannot be distinguished from the other noises in the vessel.

Only bubbles creating sound will be measured in a distribution, and this is an important factor when validating the technique discussed in the following section and assessing its applications. It is therefore necessary to understand what exactly causes the bubbles to oscillate so that the significance of the bubble size distribution can clearly be understood. It can be seen from spectrum B in Figure 7 that bubble sound is occurring before the onset of turbulence in the vessel and this sound increases as more bubbles are broken up. It seems, therefore, that the bubbles are excited into volume oscillation immediately after their formation at the impeller. However, Pumphrey and Ffowcs Williams (1990) and Pandit et al. (1992) have proposed that turbulence could reexcite bubble oscillation at their natural frequencies and that this may also be occurring when turbulent conditions exist in the vessel. The few experiments investigating the effect of turbulence (Pumphrey and Ffowcs Williams, 1990; Kolaini and Gourmilevski, 1997) show that turbulence-excited oscillations are of smaller magnitude and occur in conditions where the bubbles are close to breakage. In an agitated vessel the system is most turbulent in the region about the impeller, the same region where bubble breakup is occurring, making it impossible to clarify if some of the sound is from bubbles reexcited into oscillation by turbulence. If the excitement mechanism is indeed bubble breakage at the tip of the cavity vortex behind the impeller, then this would mean the bubble-size distributions calculated from the sound spectrum would be specifically for the bubbles formed at the impeller.

Modeling of Sound Production at the Impeller

In order to calculate bubble-size distributions from sound spectra measured in the vessel, it must be confirmed that the bubbles do oscillate at frequencies dependent on their size, calculated from Eq. 1. A model, proposed by Loewen and Melville (1991) for sound production in a breaking sea wave, has been adapted for the case of the agitated vessel for predicting the sound spectrum from measured bubble-size distributions. Modeled results were then compared with experimental sound measurements.

In the model, it is assumed that

1. Each bubble oscillates at its natural frequency in a free field calculated by Eq. 1;
2. The magnitude of each pressure pulse produced by a bubble oscillates in a damped, sinusoidal manner according to Eq. 2;
3. The pulses occur randomly with time, and the number of oscillations per unit time was estimated from pressure–time measurements;
4. The overall pressure–time trace is the summation of all the individual pulses;
5. The sound radiated by a neighboring bubble has a negligible effect on an individual pressure pulse;
6. The size distribution of the bubbles creating sound is the same as photographically measured distributions in the impeller region.

The initial pressure-peak magnitude, p_0, required for Eq. 2, was estimated from the best fit line to the scatter plot shown in Figure 4. Also included in the model are sine waves to account for pressure fluctuations at the blade-passing frequency and its second fundamental shown in Figure 6. Low-frequency noise from general turbulence is not included in the model.

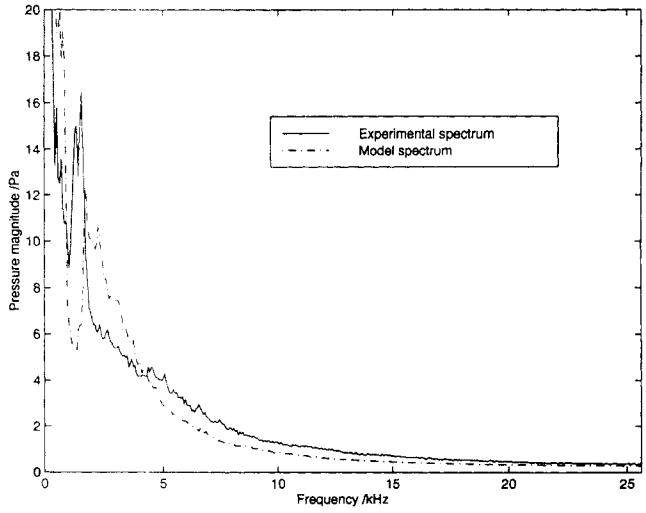

Figure 8. Modeled sound spectrum and experimentally measured sound spectrum ($N = 800$ rpm, $Q = 300$ cm$^3\cdot$min^{-1}).

Figure 8 shows a comparison between experimental sound spectrum for $N = 800$ rpm and $Q = 300$ cm$^3\cdot$min^{-1} and modeled sound spectrum based on the photographically measured bubble-size distribution. The model predicts sound at frequencies approximately 25% higher than that measured experimentally. Equation 1 predicts the frequency of a bubble oscillating in a free field away from surfaces. This free field does not exist in such a small vessel as that used in these experiments, where several rigid surfaces like the impeller blades and vessel wall are very close to the bubbles being formed. Strasberg (1953) and Devin (1961) have shown that a single, flat, rigid boundary in the close proximity of an oscillating bubble can reduce its frequency of oscillation by 20%. This reduction in the frequency of the bubble-volume oscillation will have to be accounted for when calculating the bubble-size distribution.

The modeled sound spectrum predicts sound pressures of the right order of magnitude, and for the purposes of demonstrating bubble sound production and that the bubble oscillations are below that of their natural frequencies the current model works well. The estimation of the initial peak pressure of the bubble pulse is based on highly scattered data (see Figure 4). Further investigations as to the causes of bubble sound in an agitated vessel are required to improve the model fit and for more accurate bubble-size distribution calculations.

Calculation of Bubble Size Directly from Measured Sound Spectra

Loewen and Melville (1991) suggest a method for calculating bubble sizes from sound spectra without having to analyze and count the individual pulses on a time trace, as this technique could not have a general application due to its slowness. If the contribution of a single bubble to a sound spectrum at its oscillating frequency is known, then the number of bubbles oscillating at this frequency can be calculated using Eq. 4 (Loewen and Melville, 1991):

$$N = \left(\frac{P}{\bar{p}}\right)^2, \tag{4}$$

where P is the measured pressure (Pa) in the sound spectrum at frequency, f (Hz), and $\bar{p}$ is the root-mean-square pressure (Pa) for a single bubble oscillating at the same frequency during a sample time period, T, given by

$$\bar{p}^2 = \frac{1}{T}\int_0^T [p_0 \sin(2\pi ft) e^{-(\pi\delta ft)}]^2\, dt. \tag{5}$$

It must be assumed that the sound spectrum is only due to bubbles oscillating at their natural frequencies and that a single bubble's contribution to the spectrum is only in a narrow frequency band about f. For every frequency making up a sound spectrum, $\bar{p}$ was calculated from Eq. 5 using p_0 values again estimated from experimental data. The estimated bubble-size distribution from the experimental sound spectra and the photographically measured size distribution are shown in Figure 9 ($N = 800$ rpm and $Q = 100$ cm$^3\cdot$min^{-1}). The reduction in oscillating frequency discussed earlier is not included in the calculation. Qualitatively, there seems to be good agreement between the two distributions with the calculated averages of the two distributions being closer than 20%. However, the distribution calculated from the sound spectrum is a much smoother distribution, and this is likely to be due to the damping of the bubble oscillations, as this spreads the bubble's contribution to a spectrum over a much broader band of frequencies than that assumed. The distribution calculated from the sound spectrum indicates a significant amount of bubbles around 0.2 mm in diameter, which were not measured in the photographs. This size of bubble was around the lower limit measurable that using the photographic technique available for these studies could measure. Differences between the two distributions could also be because the bubble-size distribution making sound in the impeller region is not the same as that measured in photographs.

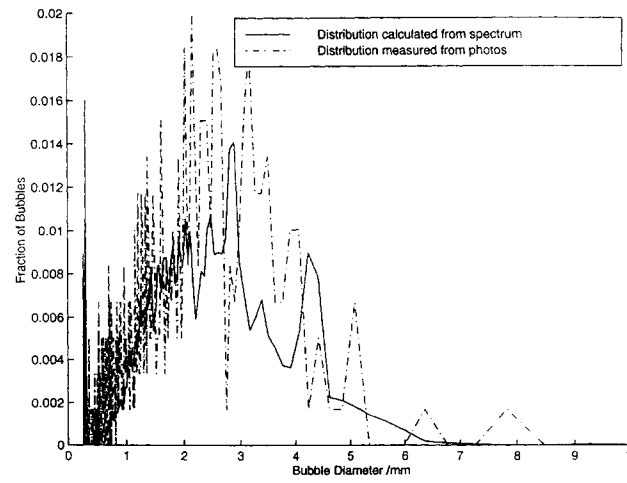

Figure 9. Bubble-size distribution calculated from experimental sound spectrum.

$N = 800$ rpm, $Q = 300$ cm$^3\cdot$min^{-1}.

There are several advantages in developing the acoustic bubble-size measurement technique further. The technique gives reasonable estimates of the average bubble size and the distribution but further investigation is required to improve accuracy. In opaque vessels, where photography is not possible, acoustic measurement will indicate significant changes in bubble size. The acoustic measurement is simple and fast. A distribution made up of over 1,000 bubbles could be measured in less than 2 min if the hydrophone signals were connected on-line to a computer. Also, smaller bubbles can be detected acoustically when compared to a basic photographic measurement technique such as the one for these studies.

Conclusions

An acoustic technique to measure the bubble-size distribution from a sound spectrum measured within an agitated vessel has been demonstrated. Experimental measurements show that measured sound pulses are due to the introduction of gas into the vessel and that these pulses are dependent on gas-bubble size. Bubble sound has been differentiated from other sound sources in the vessel. Below 700 Hz, sound is due to the impeller blades passing the hydrophone, the large gas cavities behind them, and the turbulent eddies. Above 900 Hz, sound is due to air bubbles oscillating at or close to their natural frequencies. After removal of the unwanted noise from the sound spectrum, a bubble-size distribution has been calculated and compares well with photographic measurements. The technique only measures bubbles that are emitting sound pulses and further work is required to clarify exactly what bubble-size distribution is being measured, although it is believed to be the bubble-size distribution local to the impeller region. Also the effects, such as the addition of solids or changes in viscosity, will have to be investigated, and the limiting range of conditions where the technique remains valid will have to be established. Bubbles between 0.1 and 7 mm in diameter were detected. The technique can be used in opaque liquids such as those found in fermenter systems and is relatively inexpensive in comparison to ultrasonic bubble-measurement techniques.

Literature Cited

Barigou, M., and M. Greaves, "Bubble Size Distributions in a Mechanically Agitated Gas-Liquid Contactor," *Chem. Eng. Sci.*, **47**, 2009 (1992a).

Bugman, G., and U. Von Stockar, "Characterizing Bubbles in Ultrasound," *Tibtech*, **7**, 166 (1989).

Chapelon, J. Y., P. M. Shankar, and V. L. Newhouse, "Ultrasonic Measurement of Bubble Cloud Size Profiles," *J. Acoust. Soc. Amer.*, **78**, 196 (1985).

Clark, N. N., and R. Turton, "Chord Length Distributions Related to Bubble Size Distributions in Multiphase Flows," *Int. J. Multiphase Flow*, **14**, 413 (1988).

De More, L. S., W. F. Pafford, and G. B. Tatterson, "Cavity Sound Resonance and Mass Transfer in Aerated Agitated Tanks," *AIChE J.*, **34**, 1922 (1988).

Devin, C., Jr., "Survey of Thermal, Radiation, and Viscous Damping of Pulsating Air Bubbles in Water," *J. Acoust. Soc. Amer.*, **31**(12), 1654 (1959).

Devin, C., Jr., "Resonant Frequencies of Pulsating Air Bubbles Generated in Short, Open Ended Pipes," *David Taylor Basin Model Reports*, Rep. 1522 (1961).

Eller, A. I., "Damping Constants of Pulsating Bubbles," *J. Acoust. Soc. Amer.*, **47**, 1469 (1970).

Greaves, M., and K. A. H. Kobbacy, "Measurement of Bubble Size Distribution in Turbulent Gas-Liquid Dispersions," *Chem. Eng. Res. Des.*, **62**, 3 (1984).

Hsi, R., M. Tay, D. Bukur, G. B. Tatterson, and G. Morrison, "Sound Spectra of Gas Dispersion in an Agitated Tank," *Chem. Eng. J.*, **31**, 153 (1985).

Kawase, Y., and M. Moo-Young, "Mathematical Models for Design of Bioreactors: Applications of Kolmogoroff's Theory of Isotropic Turbulence," *Chem. Eng. J.*, **43**, B19 (1990).

Kolaini, A. R., and L. A. Crum, "Observations of Underwater Sound from Laboratory Breaking Waves and the Implications Concerning Ambient Noise in the Ocean," *J. Acoust. Soc. Amer.*, **96**, 1755 (1994).

Kolaini, A. R., and A. G. Goumilevski, "Acoustic Characterization of an Adult Bubble Injected into a Fully Developed Turbulent Flow Field," *J. Acoust. Soc. Amer.*, **101**, 218 (1997).

Leighton, T. G., R. J. Lingard, A. J. Walton, and J. E. Field, "Acoustic Bubble Sizing by Combination of Subharmonic Emissions with Imaging Frequency," *Ultrasonics*, **29**, 319 (1991).

Leighton, T. G., D. G. Ramble, and A. D. Phelps, "The Detection of Fethered and Rising Bubbles Using Multiple Acoustic Techniques," *J. Acoust. Soc. Amer.*, **101**, 2626 (1997).

Leighton, T. G., and A. J. Walton, "An Experimental Study of the Sound Emitted from Gas Bubbles in a Liquid," *Eng. J. Phys.*, **8**, 98 (1987).

Loewen, M. R., and W. K. Melville, "A Model of the Sound Generated by Breaking Waves," *J. Acoust. Soc. Amer.*, **90**, 2075 (1991).

Longuet-Higgins, M. S., "Nonlinear Damping of Bubble Oscillations by Resonant Interaction," *J. Acoust. Soc. Amer.*, **91**, 1414 (1992).

Lu, W. M., R. C. Hsu, W. C. Chien, and L. C. Lin, "Measurement of Local Bubble Diameters and Analysis of Gas Dispersion in an Aerated Vessel with Disk-turbine Impeller," *J. Chem. Eng. Jpn.*, **26**, 551 (1993).

Lu, W. M., and L. C. Lin, "Gas Dispersion and Bubble Size Distribution in Dual Impeller Stirred Vessels," *J. Chin. Inst. Chem. Eng.*, **26**, 119 (1995).

Machon, V., A. W. Pacek, and A. W. Nienow, "Bubble Sizes in Electrolyte and Alcohol Solutions in a Turbulent Stirred Vessel," *Trans. Inst. Chem. Eng.*, **75A**, 339 (1997).

Manasseh, R., "Acoustic Sizing of Bubbles at Moderate to High Bubbling Rates," World Conf. on Experimental Heat Transfer Fluid Mechanics and Thermodynamics, Brussels (1996).

McClements, D. J., "Ultrasonic Characterisation of Foods and Drinks: Principles, Methods, and Applications," *Crit. Rev. Food Sci. Nutr.*, **37**, 1 (1997).

Medwin, H., and M. M. Beaky, "Bubble Sources in the Knudsen Sea Noise Spectra," *J. Acoust. Soc. Amer.*, **86**, 1124 (1989).

Minnaert, M., "On Musical Air-Bubbles and the Sounds of Running Water," *Philos. Mag.*, **16**, 235 (1933).

Nicholas, M., R. A. Roy, L. A. Crum, H. Oguz, and A. Prosperetti, "Sound Emissions by a Laboratory Cloud," *J. Acoust. Soc. Amer.*, **95**, 3171 (1994).

Pandit, A. B., J. Varley, R. B. Thorpe, and J. F. Davidson, "Measurement of Bubble Size Distribution: An Acoustic Technique," *Chem. Eng. Sci.*, **47**, 1079 (1992).

Plesset, M. S., and A. Prosperetti, "Bubble Dynamics and Cavitation," *Annu. Rev. Fluid Mech.*, **9**, 145 (1977).

Pumphrey, H. C., and J. E. Ffowcs Williams, "Bubbles as Sources of Ambient Noise," *IEEE J. Oceanic Eng.*, **OE-15**, 268 (1990).

Saxena, S. C., D. Patel, D. N. Smith, and J. A. Ruether, "An Assessment of Experimental Techniques for the Measurement of Bubble Size in a Bubble Slurry Reactor as Applied to Indirect Coal Liquefaction," *Chem. Eng. Commun.*, **63**, 87 (1988).

Strasberg, M., "The Pulsation Frequency of Non-Spherical Gas Bubbles in Liquids," *J. Acoust. Soc. Amer.*, **25**, 536 (1953).

Strasberg, M., "Gas Bubbles as Sources of Sound in Liquids," *J. Acoust. Soc. Amer.*, **28**, 20 (1956).

Stravs, A. A., and U. Von Stockar, "Measurement of Number and Size Distributions of Reflecting Objects by Pulsed Ultrasound," *J. Acoust. Soc. Amer.*, **77**, 1419 (1985).

Stravs, A. A., A. Pittet, U. Von Stockar, and P. J. Reilly, "Measurement of Interfacial Areas in Aerobic Fermentations by Ultrasonic Pulse Transmission," *Biotechnol. Bioeng.*, XXVII, 1302 (1986).

Stroud, J. S., and P. L. Marston, "Optical Detection of Transient Bubble Oscillations Associated with the Underwater Noise of Rain," *J. Acoust. Soc. Amer.*, **94**, 2788 (1993).

Sutter, T. A., G. L. Morrison, and G. B. Tatterson, "Sound Spectra in an Aerated Agitated Tank," *AIChE J.*, **33**, 668 (1987).
Updegraff, G. E., and V. C. Anderson, "Bubble Noise and Wavelet Spills Recorded 1m Below the Ocean Surface," *J. Acoust. Soc. Amer.*, **89**, 2264 (1991).
Usry, W. R., G. L. Morrison, and G. B. Tatterson, "On the Interrelationship Between Mass Transfer and Sound Spectra in an Aerated Agitated Tank," *Chem. Eng. Sci.*, **42**, 1856 (1987).
Vagle, S., and D. M. Farmer, "The Measurement of Bubble Size Distributions by Acoustic Backscatter," *J. Atmos. Oceanic Technol.*, **9**, 630 (1992).
Yoon, S. W., L. A. Crum, A. Prosperetti, and N. Q. Lu, "An Investigation of the Collective Oscillations of a Bubble Cloud," *J. Acoust. Soc. of Amer.*, **89**, 700 (1991).

Manuscript received Feb. 9, 1998, and revision received May 20, 1998.